JOURNAL OF MARITIME RESEARCH

SPECIAL ISSUE (2026) pp 273–280

ISSN: 1697-4840, www.jmr.unican.es

Robust Marine Propulsion Performance Forecasting Using Robust Heterogeneous Graph Transformer Network Model

Dr. Thomas Thangam[1,*], Capt. Kais Ali Hassan[2]

ARTICLE INFO

Special Issue:
1st International Maritime and Logistics Conference;
February 10-11, 2026.
National University of Science & Technology (NU), Oman

Article history:
Received 15 Feb 2026;
in revised from 24 Feb 2026;
accepted 05 Jun 2026.

Keywords:
Marine Vessel, Heterogeneous Graph Transformer Network, Heterogeneous Mutual Attention, Heterogeneous Message Passing.

ABSTRACT

Precise assessing of marine engine performance under dynamic load circumstances is significant for modern marine vessels to ensure fuel efficiency, operational dependability and preventative maintenance. In this paper a Robust Heterogeneous Graph Transformer Network (HGTN) is proposed for predicting marine engine performance under dynamic load variations. The raw data incorporates load-dependent indicators, engine log histories, and raw high-frequency sensor readings. The heterogeneous graph nodes characterize engine subsystems, operational parameters; edges encode their correlations and dynamic connections. The HGTN uses multi-type attention and adaptive meta-path learning to capture nonlinear effects arising from fuel injection variability, turbocharger dynamics, thermal fluctuations, and shaft load changes. The proposed HGTN technique accurately predicts brake power, SFOC, exhaust temperature, and vibration signatures, attaining an MSE of 0.0052, RMSE of 0.0719, MAE of 0.032, and R^2 of 98%. Results confirm the structure efficiency in identifying performance degradation and improving engine tuning strategies.

1. Introduction.

Maritime transport is the primary approach of worldwide trade, valued for its high cargo capacity, low transportation cost, and extensive range (Liu et al., 2025). Consequently, all-electric ship technology continues to grow, the electrical propulsion method (Stavroulakis et al., 2025; Chen et al., 2025). At the same time, the shipping industry (Kiouvrekis et al., 2025) is increasingly developing best practices and strategic guidelines to support a transition toward more sustainable operations (Thanaraj et al., 2024). Additionally, the regulatory bodies and industry organizations is crucial for ensuring that this shift toward greener maritime practices occurs in a coordinated and effective manner (Li et al., 2023; Liu et al., 2024). In (Xie et al., 2022), a hybrid ResNet–BiLSTM model is proposed for electric drive fault diagnosis. Although effective, this method weights high computational resources and long training times. Similarly, (Zaman et al., 2023) integrates multiple motion features for AIS-based waypoint detection but still shows limited generalization when encountering unseen trajectory patterns. Furthermore, encoder–decoder recurrent neural networks (Capobianco et al., 2021) trained on historical trajectory data are used to forecast prospect vessel movements. Nonetheless, it suffers to capture long-range dependencies in highly dynamic situations, foremost to concentrated estimate accurateness.

[1]Assistant Professor, Department of Process Engineering, International Maritime College Oman, Sohar, Sultanate of Oman.

[2]Lecturer, Department of Marine Engineering, International Maritime College Oman, Sohar, Sultanate of Oman.

[*]Corresponding author: Thomas Thangam. E-mail Address: thomas.thangam@imco.edu.om.

1.1. Literature Review.

Table 1: Literature review.

AUTHOR & REF.	TECHNIQUES USED	ADVANTAGES	LIMITATION
Jiang et al (2023) (Jiang et al., 2023)	Transformer –Long Short Term Memory (LSTM) for trajectory prediction	LSTM layers recollect temporal memory and smooth out noisy sequential data, providing stable short-term dynamics.	Transformers perform best with large datasets; small trajectory datasets lead to over fitting.
Jiang et al (2025) (Jiang et al., 2025)	To predict ship speed accurately Deep convolutional network prediction model is constructed and trained.	They efficiently process complex sensor data, satellite inputs, sea-state maps, and multi-channel time-series without manual feature engineering.	Difficult to explain a particular speed prediction that is made important for maritime safety and trust.
Jing et al (2024) (Jing et al., 2024)	DFFormer is a new Transformer structure developed to enhance control factor prediction in underwater gliders	Transformer backbone models global temporal interactions in glider measurements, improving prediction under ocean conditions.	DFFormer need wide labeled datasets, which is difficult to collect in underwater missions.
Ge et al (2024) (Ge et al., 2024)	Generative Adversarial Networks (GANs) with LSTM networks to accurately forecast ship speed	LSTM effectively absorbs temporal patterns in ship navigation data, whereas GAN-enhanced features boost prediction performance.	GANs are difficult to train due to instability between the generator and discriminator, increasing overall training difficulty.
Chen et al (2025) (Chen et al., 2025)	Convolutional Neural Network and Transformer used to detect the ship.	Transformers use self-attention to understand long-range dependencies, detect ships even in cluttered maritime environments.	CNNs and Transformers require significant GPU resources, detection harder on edge devices.

Source: Authors.

1.2. Problem Statement.

Existing predicting techniques suffer to capture the complex nonlinear relationships among multi-source engine parameters, sensor data, and operational states. The quick detection of performance degradation becomes challenging, reducing the effectiveness of maintenance and tuning strategies. For these issues, a HGTN this proposes that absorbs categorized correlations across diverse engine subsystems, exact prediction like brake power, SFOC, exhaust gas temperature, and vibration signatures.

1.3. Research Layout.

Remaining section II covers proposed structure description; section III contain result as well as its discussion and section IV concludes the article.

1.4. Research Contribution.

- Data preprocessing based transforms raw, noisy sensor streams and engine records into a heterogeneous graph.
- Multi-type attention and adaptive meta - path attention mechanisms is used to capture complex interactions between dissimilar types of nodes.
- HGTN is proposed to attains reliable forecast of serious operational constraints like brake power, Specific Fuel Oil Consumption (SFOC), exhaust gas temperature, and vibration signatures.

2. Proposed System Description.

The block diagram for proposed work is shown in figure 1, using HGTN to enhance the accurateness of marine engine performance forecasting under load conditions. At first data pre-processing accumulate load-dependent performance metrics, historical engine logs and raw sensor evaluations from onboard monitoring structures. The heterogeneous graph, nodes signify engine subsystems, operational modes and physical parameters, whereas edges encode their correlations and interactions. To ensure data dependability noise reduction, normalization, and extraction of temporal–statistical features are also performed.

Figure 1: Proposed block diagram.

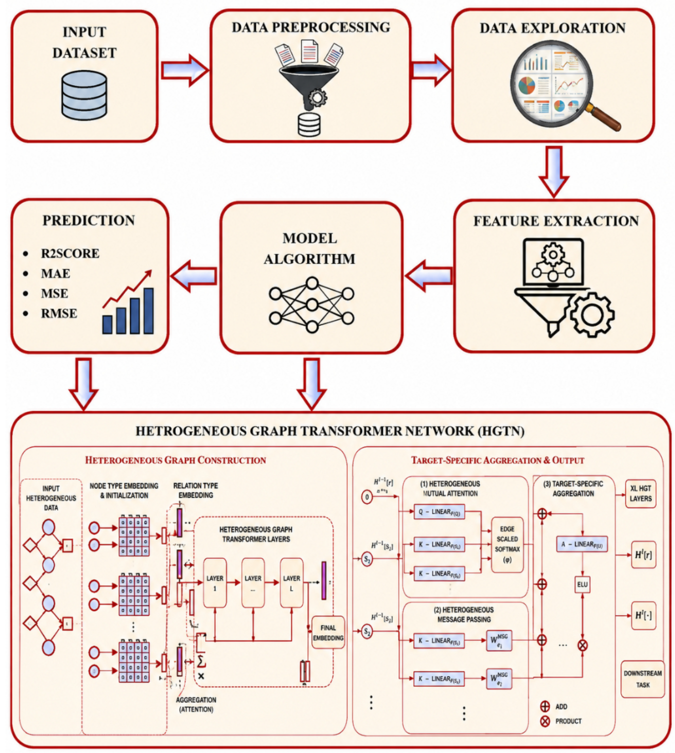

Source: Authors.

HGTN architecture controls multi - type attention mechanisms to nonlinear behavior arising from fuel injection variability, turbocharging dynamics, thermal fluctuations, and shaft load variations. By adaptive meta-path attention, the network acquires hierarchical relationships across diverse node groups and recognizes patterns of performance degradation.

2.1. Data Pre-Processing.

Data pre-processing accumulates information under different marine engine operating conditions with multiple onboard monitoring systems to support propulsion performance forecasting. High-frequency sensor data attained from the Engine Monitoring System (EMS) contain temperature, pressure, vibration, acoustic signals, flow rate, and electrical parameters. The collected data are then coordinated using unified timestamps, clock correction, and interpolation to ensure temporal consistency. The noise filtering and data quality validation are performed to remove sensor drift, diminish measurement errors, and develop the dependability of the dataset.

2.2. Data Exploration.

For forecasting marine propulsion, the pre-processing module constructs a heterogeneous graph by identifying objects like engine subsystems, operational modes, then physical parameters, and representing each as distinct node types. Here the edges are generated to encode important relationships, containing sensor-to-subsystem dependencies, parameter co-variation patterns, and dynamic interactions observed under different load states. After that noise-reduction filters and smoothing techniques are applied to eliminate spikes, sensor drift, and inconsistent depths. Then it normalizes the different sensor from the data and the temporal-statistical are extracted to capture the engine dynamic over time. Followed by the cleaned information forms a heterogeneous graph structure fed to HGTN architecture.

2.3. Feature Extraction by Heterogeneous Graph Transformer Network.

The proposed HGTN architecture for marine propulsion forecasting controls the meta-relations within a heterogeneous graph to monitor the learning process. Here HGTN parameter have separate weight matrices for each node, edge node type combination, allowing type-aware attention, message passing, and information propagation. This method allows capturing different interaction patterns then structural semantics of heterogeneous data more efficiently.

2.3.1. Heterogeneous Graph in Marine System.

In marine propulsion forecasting, engine behavior is inclined through many interacting components like fuel systems, turbochargers, cooling circuits, sensors, operational modes, and environmental conditions. These interfaces certainly form a heterogeneous graph, where: Every node denotes a different type of engine object as well as every edge denotes a exact relationship, such as fuel–air coupling, thermal transfer, vibration–load correlation, or operational transitions. HG is well-defined as an absorbed graph which is denoted by [all equation in Heterogeneous Graph Transformer]:

$$G = (V, E, L, M) \tag{1}$$

Wherever, every node $v \in V$and every edge by $e \in E$ are related through their nature plotting utilities.

$$\tau(v) : V \to L \tag{2}$$

$$\varphi(e) : E \to M \tag{3}$$

Moreover, to more accurately represent heterogeneous networks, this permit the possibility of multiple relation types existing between the same pair of nodes.

2.3.2. Meta-Relations in Marine Propulsion.

In this for a communication between a source node s as fuel pressure sensor and a target node t , as brake power output.

$$e = (s, t) \tag{4}$$

$$\langle \tau(s), \phi(e), \tau(t) \rangle \tag{5}$$

Here $\tau(\cdot)$ symbolizes the node type and $\phi(e)$ indicates the relation type. The inverse relation is denoted as $\phi(e)^{-1}$.

2.3.3. Overall HGT Architecture for Marine Propulsion.

For forecasting heterogeneous graph representing an engine state, HGT process all pairs of linked nodes like source and the target. In the source node there is a temperature sensor, vibration, fuel injector and in the target node there is a brake power, SFOC, exhaust temperature. For each target node model aggregates data as of source nodes to compute updated, contextualized embedding. Fig. 2 shows the design of HGN and fig. 3 shows structure of HGTN.

Figure 2: Architecture of HGN.

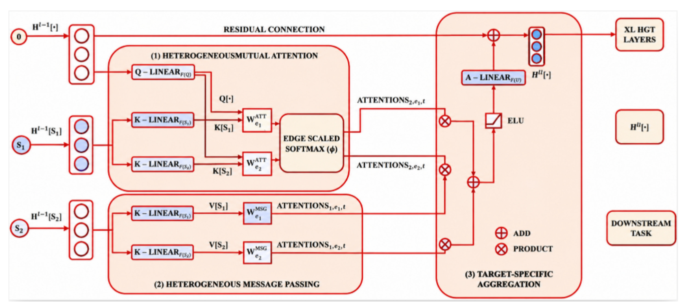

Source: Authors.

Figure 3: Structure of HGTN.

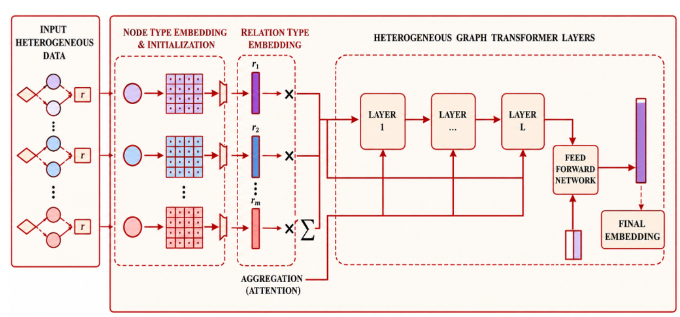

Source: Authors.

The heterogeneous mutual attention computes the type - aware attention strength between engine components. Also a target specific aggregation aggregates message using attention weights and map them back to target node distributions.

2.3.4. Heterogeneous Mutual Attention for Marine Engine Data.

Marine propulsion systems contain diverse feature distributions temperature sensors differ from pressure sensors and operational modes. GNN attention (like GAT) assumes the same feature space,

$$H^l(t) = \underset{\forall s \in N(t), \forall e \in E(s,t)}{\text{Aggregate}} (\text{Attention}(s,t) \cdot \text{Message}(s)) \quad (6)$$

In this case, Attention shows every source node position,

$$\text{Attention}_{HGT}(s,t) = \underset{\forall s \in N(t)}{\text{softmax}} \left(\Big\|_{i \in [1,h]} \text{ATT-head}^i(s,e,t) \right) \quad (7)$$

$$\text{ATT-head}^i(s,e,t) = \left(K^i(s) W^{ATT}_{\phi(e)} Q^i(t)^T \right) \cdot \frac{\mu \langle \tau(s), \phi(e), \tau(t) \rangle}{\sqrt{d}} \quad (8)$$

$$K^i(s) = K\text{-Linear}^i_{\tau(s)} \left(H^{(l-1)}[s] \right) \quad (9)$$

$$Q^i(t) = Q\text{-Linear}^i_{\tau(t)} \left(H^{(l-1)}[t] \right) \quad (10)$$

Where Eqns. 9 and 10 evaluate how closely the query vector $Q^i(t)$ aligns with the key vector $K^i(s)$. Every source node s is projected using a type-specific linear transformation $K^{Linear}_{\tau(s)}$, ensuring that nodes of different types retain their unique feature distributions. Similarly, the target node t is mapped into the i^{th} query vector through its corresponding type-dependent projection $Q^{Linear}_{\tau(t)}$.

2.3.5. Heterogeneous Message Passing.

To estimate the message passing the source node to the target node it is expressed as:

$$\text{Message}_{HGT}(s,e,t) = \Big\|_{i \in [1,h]} \text{MSG-head}^i(s,e,t) \quad (11)$$

$$\text{MSG-head}^i(s,e,t) = M\text{-Linear}^i_{\tau(s)} \left(H^{(l-1)}[s] \right) W^{MSG}_{\phi(e)} \quad (12)$$

Where i^{th} communication through its $MSG\text{−}head^i\,(s,e,t)\ h$ message heads to get $\text{Message}_{HGT}(s,e,t)$ for every node brace.

2.3.6. Target-Specific Aggregation.

For this aggregation once the dissimilar multi-head attention scores as well as messages are computed, they aggregated from all source nodes as well as integrated into the target node to update its representation.

$$\widetilde{H}^l[t] = \underset{\forall s \in N(t)}{\oplus} (\text{Attention}_{HGT}(s,e,t) \cdot \text{Message}_{HGT}(s,e,t)) \quad (13)$$

$$H^{(l)}[t] = \sigma \left(A\text{-Linear}_{\tau(t)} \widetilde{H}^l[t] \right) + H^{(l-1)}[t] \quad (14)$$

It handles multi - sensor, multi-system coupling found in diesel engines, propulsion systems, and auxiliary machinery. And the method is nonlinear dependency between fuel systems, air systems, thermal systems, and environmental factors. It supports meta-relation–based attention, essential for understanding load-induced changes.

3. Results and Discussion.

In this section the proposed HGT model is used to for marine propulsion forecasting. Using condition-based-monitoring-in-marine-system dataset from kaagle.com the dataset is taken and utilized in Python software. Its dataset shape contains 12434 rows and 18 columns then it is split as 20% for test and 80% for train.

Table 2: Parameters for the transformer model.

Parameter	Value
Epochs	30
Dropout	0.3
Learning rate	0.001
Filters	64
Layers	2 GCN + 1 Transformer block
Optimizer	Adam
Loss	Regression
Num. of heads	8
FFN dimension	2048
Activation	ReLU

Source: Authors.

Table 2 shows the parameter and its value of the transformer model. It have the Epochs value of 30, dropout is 0.3, learning rate of 0.001 and filters of 64.

Figure 4: Dataset columns.

```
DATASET COLUMNS:

Lever position
Ship speed (v)
Gas Turbine (GT) shaft torque (GTT) [kN m]
GT rate of revolutions (GTn) [rpm]
Gas Generator rate of revolutions (GGn) [rpm]
Starboard Propeller Torque (Ts) [kN]
Port Propeller Torque (Tp) [kN]
Hight Pressure (HP) Turbine exit temperature (T48) [C]
GT Compressor inlet air temperature (T1) [C]
GT Compressor outlet air temperature (T2) [C]
HP Turbine exit pressure (P48) [bar]
GT Compressor inlet air pressure (P1) [bar]
GT Compressor outlet air pressure (P2) [bar]
GT exhaust gas pressure (Pexh) [bar]
Turbine Injecton Control (TIC) [%]
Fuel flow (mf) [kg/s]
GT Compressor decay state coefficient
GT Turbine decay state coefficient
```

Source: Authors.

Figure 4 displays the dataset columns. It shows the lever position, ship speed, gas turbine, gas generator, propeller etc.

Figure 5: Distribution of fuel flow.

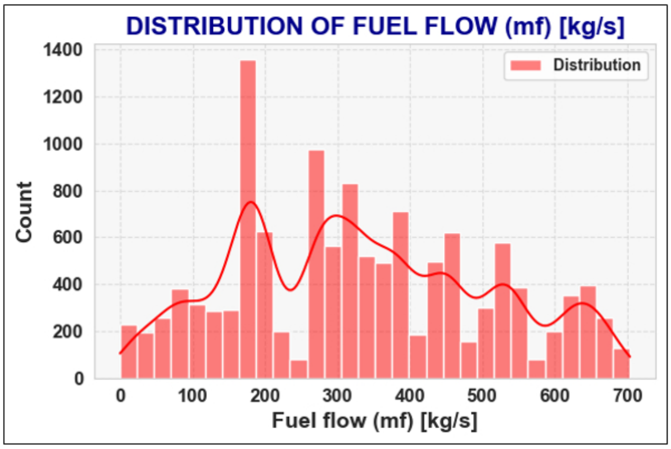

Source: Authors.

Figure 5 displays the distribution of fuel flow rates, the maximum values fall between 150–350 kg/s through noticeable peaks around 200 kg/s. The red curvature highlights the overall drift, signifying multiple operating conditions and variations in engine fuel consumption.

Figure 6: Comparison of GT decay state coefficients.

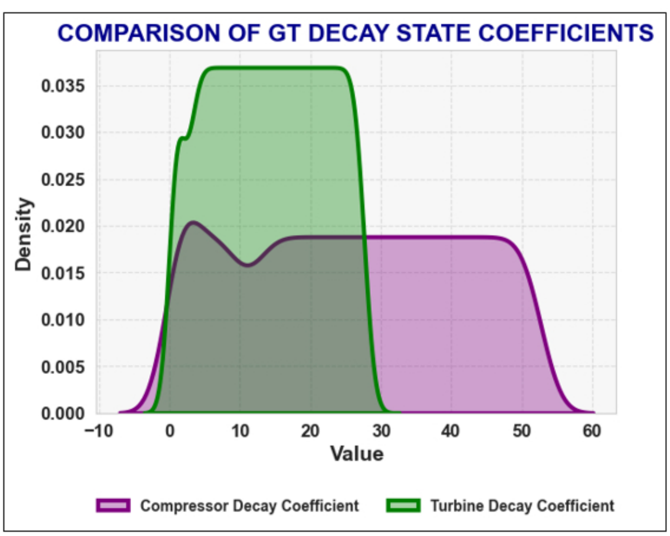

Source: Authors.

Figure 6 shows compressor and turbine decay a coefficient, presenting that compressor decay extents across a wider range of values, whereas turbine decay is concentrated mainly among 5 and 30. This displays that turbine drop is more closely distributed, whereas compressor degradation varies more across operating conditions.

Figure 7: Distribution comparison of GT compressor inlet and outlet pressure.

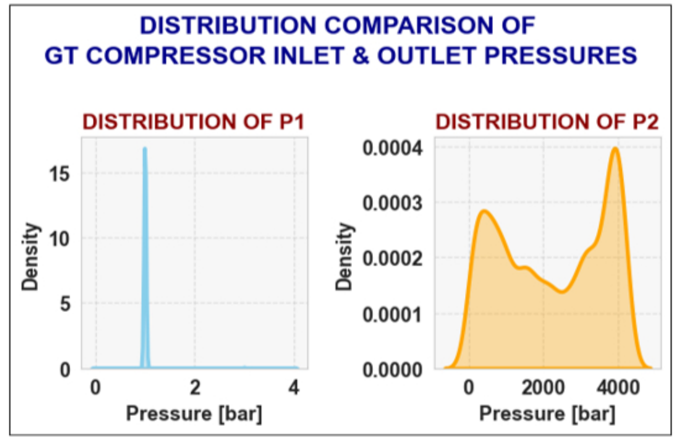

Source: Authors.

Figure 7 demonstrate the distribution comparison of GT compressor inlet as well as outlet pressure. The inlet pressure P1 demonstrates an extremely narrow distribution around a single low-pressure value, demonstrating highly constant compressor access conditions. Then the outlet pressure P2 spans a wide range with multiple density peaks, reflecting varying operating loads and dynamic compressor discharge behaviour.

Figure 8: Train-test split counts.

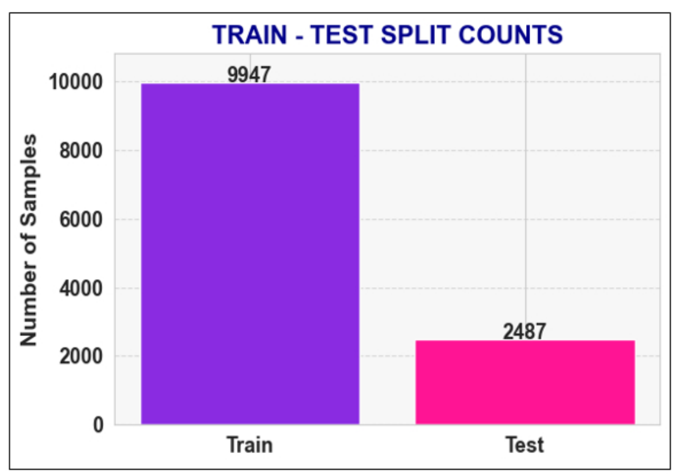

Source: Authors.

Figure 8 displays the train-test split counts. The total number of samples is 10000 in that train have 9948 samples and tests have 2487 samples.

Figure 9 displays the model loss. In that together training as well as validation loss falls suddenly throughout the first few epochs, showing quick learning. Then, the curves converge smoothly near zero, indicating stable training with no signs of over fitting.

Figure 9: Model loss.

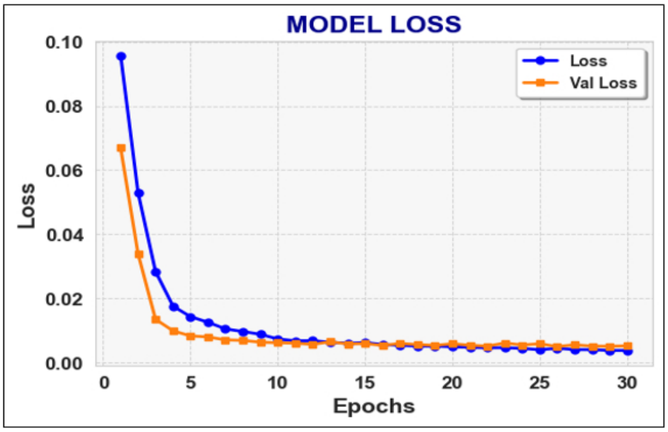

Source: Authors.

Figure 10: Model MAE.

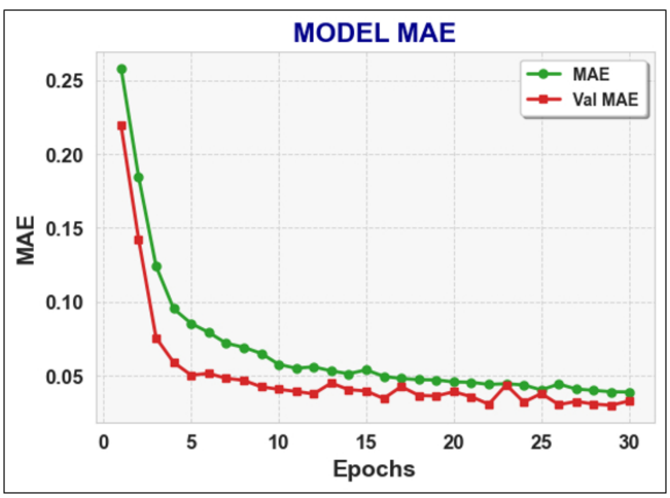

Source: Authors.

Figure 11: Error distribution.

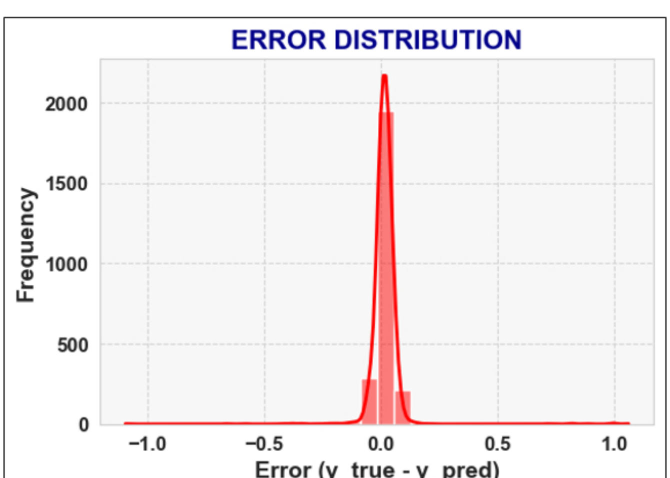

Source: Authors.

Figure 10 shows the model MAE. It displays a rapid decrease in training as well as validation error through the early epochs, specifying fast model convergence. Then both stabilize at low values with the validation MAE consistently lower, reflecting strong performance.

Figure 11 shows the error distribution it is sharply centered on zero, indicating that the predicted values closely match the true values with minimal deviation. Then there is a narrow spread demonstrations low variance in prediction errors, checking high model accuracy and stability.

Figure 12: Error metrics.

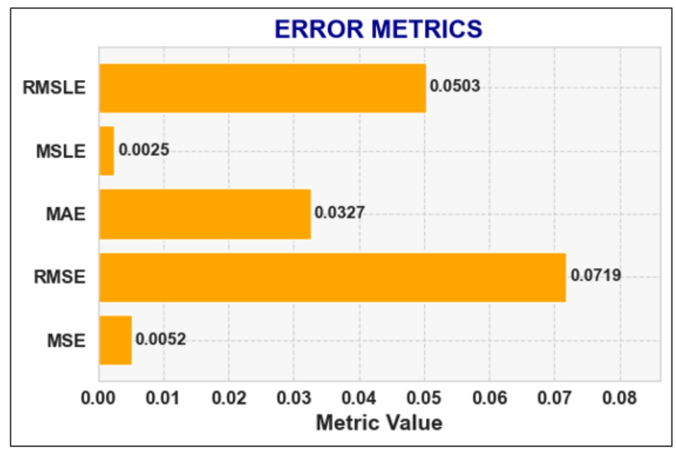

Source: Authors.

Figure 12 shows the error metrics, it have the RMSLE OF 0.0503, MSLE OF 0.0025, MAE OF 0.032, RMSE OF 0.0719 and MSE of 0.0052.

Figure 13: Actual vs predicted values.

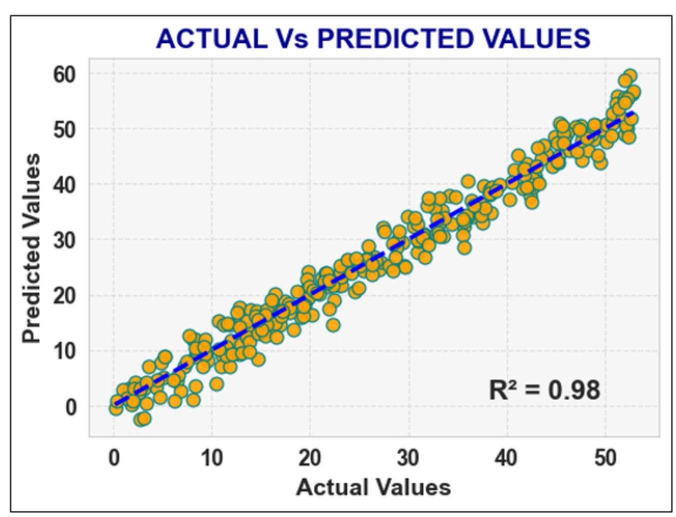

Source: Authors.

Figure 13 displays the actual vs predicted values. The proposed HGTN have the R^2 value of 0.98.

3.1. Ablation Study.

In the comparison table 3 the MSE, RMSE and MAE values are compared. TRFM-LS (Jiang et al., 2023) have the MAE of 1.22, RMSE of 1.58, DFFormer (Jing et al., 2024) have the MAE of 0.96 and RMSE of 1.1, Deep convolutional network (Jiang et al., 2025) have the MAE of 0.2, MSE of 0.12 and RMSE of 0.3, Generator-LSTM (Chen et al., 2025) have the MAE of 0.16, MSE of 0.05 and RMSE of 0.24 and the proposed HGTN have the MAE of 0.032, MSE of 0.005 and RMSE of 0.071 respectively.

Table 3: Comparison of MSE, RMSE and MAE.

Author & Ref	MAE	MSE	RMSE
Jiang et al (Jiang et al., 2023)	1.229	-	1.58
Jing et al (Jing et al., 2024)	0.96	-	1.1
Jiang et al (Jiang et al., 2025)	0.2	0.1	0.3
Chen et al (Chen et al., 2025)	0.16	0.05	0.24
Proposed work	0.032	0.005	0.071

Source: Authors.

Figure 14: Comparison of R^2.

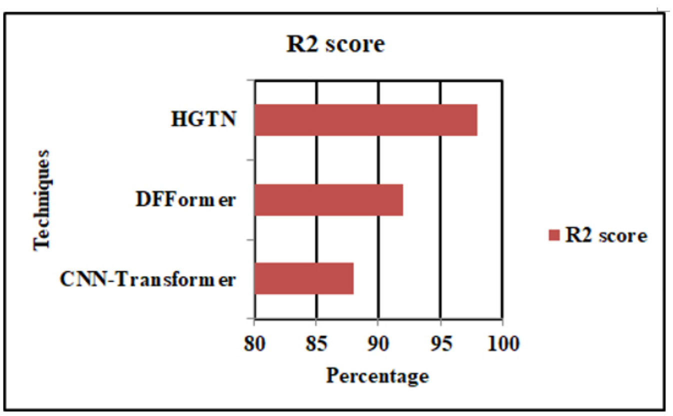

Source: Authors.

Figure 14 shows the evaluation of R^2. CNN-Transformer (Ge et al., 2024) of 88%, DFFormer (Jing et al., 2024) of 92% and the proposed HGTN of 98% which is high compared to the existing method respectively.

Conclusions.

This paper, proposed an HGTN-based framework that effectively models complex marine engine behaviour by incorporating multi-source sensor data into a unified heterogeneous graph structure. The data pre-processing phase transforms raw, noisy sensor streams and engine logs into a heterogeneous graph. This graph encodes engine subsystems, physical parameters, and operational modes. Its adaptive attention mechanisms accurately capture nonlinear interactions, allowing precise forecasting of key performance metrics and quick recognition of degradation. With strong evaluation results of MSE 0.0052, RMSE 0.0719, MAE 0.032, R^2 98%, the system provides a reliable decision-support tool for improving fuel efficiency, operational reliability, and predictive maintenance in modern marine vessels.

Acknowledgment.

The authors gratefully acknowledge the support of the International Maritime College Oman, Sultanate of Oman, for providing research facilities.

References.

Liu, Y., Xiong, W., Chen, N., & Yang, F. (2025). VTLLM: A Vessel Trajectory Prediction Approach Based on Large Language Models. *Journal of Marine Science and Engineering*, 13(9), 1758.

Stavroulakis, P.J., Prousaloglou, P., Kyriakopoulou-Roussou, M.C., & Papadimitriou, S. (2025). AI-driven data mining for sustainable ship power system technologies. *Transportation Engineering*, 100383.

Chen, Y., Chen, H., Jiang, Y., Wang, C., Wang, N., Zhang, F., & Zhang, Z. (2025). DriftNet: target-area differential attention mechanism for marine drifter trajectory prediction. *Engineering Applications of Computational Fluid Mechanics*, 19(1), 2563083.

Kiouvrekis, Y., Gkirtzou, K., Zikas, S., Kalatzis, D., Panagiotakopoulos, T., Lajic, Z., Papathanasiou, D., & Filippopoulos, I. (2025). An Explainable Machine Learning Approach for IoT-Supported Shaft Power Estimation and Performance Analysis for Marine Vessels. *Future Internet*, 17(6), 264.

Thanaraj, M.S., Poomalai, R., Vibin, R., Kamalakar, V., Gupta, S., Perumal, M.P.R., & Vadivel, M. (2024). Sustainable energy integration for seawater desalination. *Journal of Environmental Protection and Ecology*, 25(6), 2086–2096.

Li, W., Zuo, Y., Su, T., Zhao, W., Ma, X., Cui, G., Wu, J., & Song, Y. (2023). Firefly Algorithm-based semi-supervised learning with transformer method for shore power load forecasting. *IEEE Access*, 11, 77359–77370.

Liu, Y., Jin, H., Yang, X., Tang, T., Song, Q., Chen, Y., Liu, L., & Jiang, S. (2024). Early fault diagnosis and prediction of marine large-capacity batteries based on real data. *Journal of Marine Science and Engineering*, 12(12), 2253.

Xie, J., Shi, W., & Shi, Y. (2022). Research on fault diagnosis of six-phase propulsion motor drive inverter for marine electric propulsion system based on Res-BiLSTM. *Machines*, 10(9), 736.

Zaman, B., Marijan, D., & Kholodna, T. (2023). Interpolation - based inference of vessel trajectory waypoints from sparse AIS data in maritime. *Journal of Marine Science and Engineering*, 11(3), 615.

Capobianco, S., Millefiori, L.M., Forti, N., Braca, P., & Willett, P. (2021). Deep learning methods for vessel trajectory prediction based on recurrent neural networks. *IEEE Transactions on Aerospace and Electronic Systems*, 57(6), 4329–4346.

Jiang, D., Shi, G., Li, N., Ma, L., Li, W., & Shi, J. (2023). TRFM-ls: Transformer-based deep learning method for vessel trajectory prediction. *Journal of Marine Science and Engineering*, 11(4), 880.

Jiang, X., Dai, Y., Li, S., Ma, R., Du, T., Zou, Y., Zhang, P., Zhang, Y., & Sun, P. (2025). Research on ship speed prediction based on time series imaging and deep convolutional network fusion method. *Applied Ocean Research*, 154, 104384.

Jing, Y., Ma, C., An, J., Li, Z., Sun, X., & Guo, W. (2024). Nonstationary Control Parameter Prediction for Underwater Gliders Utilizing an Innovative Transformer-Based Model. *Journal of Marine Science and Engineering*, 12(11), 2106.

Ge, X., Li, X., Zhang, C., Li, J., & Gao, Y. (2024). Robust and real-time ship object detection method based on enhanced CNN. *IEEE Access*, 12, 112196–112210.

Chen, X., Wu, P., Zhang, Y., Wang, X., Xian, J., & Zhang, H. (2025). Smart Maritime Transportation-Oriented Ship-Speed Prediction Modeling Using Generative Adversarial Networks and Long Short-Term Memory. *Journal of Marine Science and Engineering*, 13(6), 1045.